

UDC 539.3

INFLUENCE OF MASS ON THE EFFICIENCY AND DYNAMICS OF SINGLE-SIDED AND DOUBLE-SIDED VIBRO-IMPACT NONLINEAR ENERGY SINKS

P.P. Lizunov**O.S. Pogorelova****T.G. Postnikova****O.V. Gerashchenko***Kyiv National University of Construction and Architecture
31, Povitryanykh Syl ave., Kyiv, Ukraine, 03680*

DOI: 10.32347/2410-2547.2024.113.3-17

The efficiency of the asymmetric single-sided and symmetric double-sided vibro-impact nonlinear energy sinks, that is, vibro-impact dampers, for mitigating unwanted vibrations of the main structure are quite high and similar for dampers with different masses and designs. However, its dynamic behavior is different. The optimal design of the dampers with lower mass has unusual, “strange” parameter set. The regions of bilateral damper impacts on the both barriers are narrow and located near the resonant frequency of the exciting force.

Keywords: nonlinear energy sink, damper, vibro-impact, single-sided, double-sided, optimization, bilateral impacts.

1. Introduction

This paper discusses the problem of mitigating undesirable vibrations of a heavy main structure. One of the ways to solve it is the use of active, hybrid and passive vibration control devices. Passive control devices have the advantage of having no additional power source. Due to the development of nonlinear methods and related software, nonlinear passive vibration control devices have been proposed after extensive discussion and application of linear devices such as Tuned Mass Dampers (TMD) [1, 2]. The devices attached to the main structure using nonlinear coupling have been widely discussed during the last two decades. They have been called Nonlinear Energy Sinks because their discussion began within the framework of the idea of Targeted Energy Transfer (TET) [3]. This idea states that such dampers, due to their nonlinearity, take away the part of the main structure energy and thus reduce its energy [4, 5].

The world scientific literature proposes many different types of NESs. The vibro-impact nonlinear energy sink (VI NES), that is, the vibro-impact damper, is one of them [6, 7, 8]. The VI NESs are considered to be a fairly effective type [9, 10, 11]. When considering the VI NES problem, finding its optimal design is of paramount importance. The optimal damper design, that is, a set of its parameters, should provide the best mitigation of the main structure vibrations. However, this task is complex and ambiguous. Optimization procedures do not and cannot give an unambiguous result, since there are many damper parameter sets that provide the similar mitigation of the main structure vibrations [12]. This article shows this phenomenon very clearly. We perform optimization procedures using standard software, namely MATLAB platform tools. It is worth noting that the optimization procedure itself allows for the great arbitrariness [13]. Its execution requires a great experience and skill from the performer.

The problem of impact modeling is an important one in studying the vibro-impact system dynamics. After detailed examining this problem [14, 15], we simulate an impact using the interactive contact force according to the quasi-static Hertz's contact theory [16, 17].

In this paper, we consider two classical types of VI NESs, namely asymmetric single-sided and symmetric double-sided (SSVI NES and DSVI NES). They differ only in geometry, more precisely the layout of the obstacles, and have the same mechanics. The system strong nonlinearity and discontinuity are due to the repeated damper impacts on the obstacles. In SSVI NES model, it hits directly the PS, which is the left barrier in its oscillatory motion, and the right obstacle. In DSVI NES model the damper hits the left and right obstacles. In the search for an optimal damper design, we do not include

its mass in the list of optimized parameters and search for an optimal set of damper parameters separately for each predetermined mass. The paper analyzes the influence of damper mass on its efficiency in mitigating the main structure vibrations and on the system dynamic behavior.

Our previous work [18] studied in detail the system dynamic behavior and the efficiency of the damper with mass 40 kg. This paper has an extensive bibliography.

So, the goals of this article are as follows:

- find the sets of optimal damper parameters for both models and for each chosen damper mass;
- compare the efficiency of both damper models in mitigating vibrations of the main structure for each chosen damper mass;
- show and compare the dynamic behavior of both damper models for each chosen mass when the exciting force frequency is changed;
- show the effect of changing the damper mass on its efficiency and system dynamic behavior.

2. Model description and governing equations

In this paper, we study the dynamic behavior of a two-mass vibro-impact system with two-degrees-of-freedom consisting of a main body (primary structure - PS) and a vibro-impact damper attached to it. We study the efficiency of the damper in mitigating the PS vibrations. The dependence of damper efficiency and system dynamic behavior on the mass of the damper with other optimized parameters is also studied. A vibro-impact damper is a nonlinear energy sink (NES). Two damper types are considered in this paper, namely asymmetric single-sided and symmetric double-sided vibro-impact NESs – SSVI NES and DSVI NES. Their conceptual schemes are presented in Fig.1. They differ only in geometry, namely in obstacle layout; the mechanical connections are the same. The symmetry of the double-sided VI NES is also only geometrical. Dampers of greater mass make symmetrical impacts on the both obstacles, but the symmetry of the impacts is broken for dampers with lower mass.

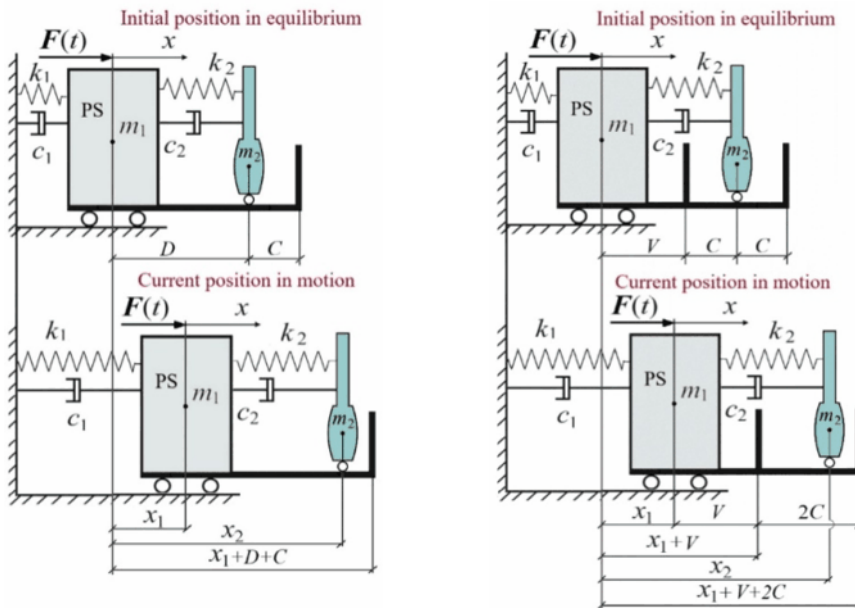


Fig. 1. Conceptual schemes of asymmetric single-sided VI NES; symmetric double-sided VI NES

The designations of mechanical connections, masses of both bodies, and distances are shown in Fig. 1. The damper mass is much less than the PS mass $m_2 \ll m_1$. The PS is under the action of an external load $F(t)$, which is a harmonic force in this paper

$$F(t) = P \cos(\omega t + \varphi_0), \quad P = 800 \text{ N. Its period is } T = 2\pi/\omega. \quad (1)$$

The parameters of the primary structure are set in advance and are not subject to optimization in this paper. We set them up as follows: $m_1 = 1000 \text{ kg}$, $k_1 = 3.95 \cdot 10^4 \text{ N/m}$, $c_1 = 452 \text{ N}\cdot\text{s/m}$.

The problem of impact modeling is very important in the study of vibro-impact system movement. After examining this problem, we in all our works simulate an impact using interactive nonlinear contact force according to quasi-static Hertz contact theory

$$F_{con}(z) = K[z(t)]^{3/2}. \quad (2)$$

The impact is not instantaneous; it has some duration. Hertz's theory allows for local deformations in the contact zone. In formula (2), z is the colliding bodies' rapprochement in the contact zone due to local deformation. This rapprochement caused by an impact may be written through distance specifications. Naturally, the rapprochements for left and right impacts are different. The left impact is a damper impact on the PS directly for SSVI NES and on the left obstacle for DSVI NES. The right impact is a damper impact on the right obstacle for both damper types.

The left impacts occur when

for SSVT NES

$$\begin{aligned} x_1 &\geq x_2, \\ \text{i.e. } (x_1 - x_2) &\geq 0 \end{aligned}$$

then the rapprochements are

$$z_1 = x_1 - x_2$$

for DSVI NES

$$\begin{aligned} x_2 &\leq (x_1 + V), \\ \text{i.e. } (x_1 - x_2 + V) &\geq 0 \end{aligned}$$

then the rapprochements are

$$z_1 = x_1 - x_2 + V.$$

The right impacts occur when

$$\begin{aligned} x_2 &\geq (x_1 + D + C), \\ \text{i.e. } (x_2 - x_1 - D - C) &\geq 0 \end{aligned}$$

$$z_2 = x_2 - x_1 - D - C$$

$$\begin{aligned} x_2 &\geq (x_1 + V + 2C), \\ \text{i.e. } [x_2 - x_1 - (V + 2C)] &\geq 0 \end{aligned}$$

$$z_2 = x_2 - x_1 - (V + 2C).$$

The coefficient K in formula (2) characterizes the mechanical and geometric properties of colliding surfaces. Therefore, it also differs for damper impacts on the left obstacle (or PS directly) and on the right obstacle:

When impacting the left obstacle (or PS directly)

When impacting the right obstacle

$$K_1 = \frac{4}{3} \frac{q_1}{(\delta_1 + \delta_2) \sqrt{A_1 + B_1}},$$

$$K_2 = \frac{4}{3} \frac{q_2}{(\delta_3 + \delta_4) \sqrt{A_2 + B_2}},$$

$$\delta_1 = \frac{1 - v_1^2}{E_1 \pi}, \quad \delta_2 = \frac{1 - v_2^2}{E_2 \pi}.$$

$$\delta_3 = \frac{1 - v_3^2}{E_3 \pi}, \quad \delta_4 = \frac{1 - v_4^2}{E_4 \pi}.$$

Here the Young's moduli of elasticity for all surfaces E_1, E_2, E_3, E_4 and Poisson's ratios v_1, v_2, v_3, v_4 are included into the characteristics of colliding surfaces. The values E_1 and v_1 characterize the contact surface of the left barrier, i.e. the PS or the left obstacle; the values E_3 and v_3 – the contact surface of the right obstacle; the values E_2, E_4 and v_2, v_4 – the left and right contact surfaces of the vibro-impact damper. We considered the values E_1, E_3 and v_1, v_3 as predetermined and did not optimize them:

$$E_1 = E_3 = 2.1 \cdot 10^{11} \text{ N/m}^2, \quad v_1 = v_3 = 0.3.$$

The values E_2, E_4 and v_2, v_4 were included in the list of optimized parameters. There were obtained the system responses to their changes. This made it possible to analyze the effect of changing the mechanical characteristics of colliding surfaces in more detail than the more prevalent consideration of the experimental restitution coefficient [19]. The results of their optimization will be shown in next Sec. 3.

Then the motion equations for this system are as follows:

$$\begin{aligned} m_1 \ddot{x}_1 + c_1 \dot{x}_1 + k_1 x_1 - c_2 (\dot{x}_2 - \dot{x}_1) - k_2 (x_2 - x_1 - D) &= F(t) - H(z_1) F_{con}(z_1) + H(z_2) F_{con}(z_2), \\ m_2 \ddot{x}_2 + c_2 (\dot{x}_2 - \dot{x}_1) + k_2 (x_2 - x_1 - D) &= H(z_1) F_{con}(z_1) - H(z_2) F_{con}(z_2). \end{aligned} \quad (4)$$

The initial conditions are

for SSVI NES

at $t = 0$, we have

$$\begin{aligned} x_1(0) &= 0, \quad x_2(0) = D, \\ \dot{x}_1(0) &= \dot{x}_2(0) = 0, \quad \varphi_0 = 0. \end{aligned}$$

for DSVI NES

at $t = 0$, we have

$$\begin{aligned} x_1(0) &= 0, \quad x_2(0) = V + C, \\ \dot{x}_1(0) &= \dot{x}_2(0) = 0, \quad \varphi_0 = 0. \end{aligned}$$

The presence of the discontinuous Heaviside step function $H(z)$ in the motion equations (4) makes the set of the Ordinary Differential Equations (ODE) stiff one. The integration step of a stiff system should not only be variable, but also extremely small at the impact points. For integrating this system, we use MATLAB stiff ODE solver *ode23s*. This variable-step solver allows us to determine with sufficient accuracy the instant when the Heaviside function $H(z)$ becomes equal to unity, that is, in our problem the collision of the bodies begins.

Integration of the motion equations (4) determines the displacements and the velocities of both bodies, which allow us to calculate the total mechanical energy of the primary structure using the well-known formula:

$$E_{total}(t) = E_{kinetic}(t) + E_{poten}(t) = \frac{m_1 \dot{x}_1(t)^2 + k_1 x_1(t)^2}{2}. \quad (5)$$

Its maximum value is chosen as the objective function for the optimization procedures.

3. Optimization of damper parameters

The world scientific literature as well as our studies and calculations insist that optimizing the damper parameters to maximize its effectiveness for mitigating the PS vibrations is a necessary and important procedure. Mitigating the PS vibrations means reducing its maximum displacements and velocities. Therefore, it is reasonable to evaluate the reduction of the maximum total mechanical energy of the PS, which is calculated by the formula (5). This evaluation is in line with the idea of Targeted Energy Transfer (TET), under which the NESs are studied. According to this idea, the NES, due to its nonlinearity, takes away some of the PS energy and consequently reduces its energy. So, it is reasonable to choose the maximum total energy of the PS E_{1max} as the objective function and search for such values of damper parameters that ensure its minimal value. In our previous work [20], we showed that the choice of parameters for its calculation is also important. It was shown that the exciting force frequency, at which the objective function is calculated, should be close to the resonant one. We calculate it at $\omega = 6.3$ rad/s.

We use standard software for minimizing the objective function, namely the *surface* and *fminsearch* programs from the MATLAB platform. Program *surface* allows us to get an initial assessment for various parameters. Program *fminsearch* searches for local minima of the objective function and allows simultaneous optimization of several parameters. Our methodology for performing optimization procedures has been described in detail in our previous papers [18, 21]. In these works, it has been shown that a softer impact provides a better reduction of E_{1max} . There were found the optimal values of the Young's moduli $E_2 = 2.21 \cdot 10^7$ N/m², $E_4 = 2.05 \cdot 10^7$ N/m², which is consistent with suggestions to use a smaller value of Newtonian restitution coefficient when recording the velocity jump using this coefficient in impact modeling [22-24].

The scientific literature often recommends including the damper mass m_2 into the list of optimized parameters. However, the optimization programs show that a larger damper mass provides a smaller objective function value for the similar values of other parameters. Table 1 summarizes these values for DSVI NES.

Table 1

The results of simultaneous optimization of five parameters for DSVI NES

V_{opt} , m	C_{opt} , m	c_{2opt} , N·s/m	k_{2opt} , N/m	m_{2opt} , kg	E_{1max} , J
0.496	0.238	64.8	217	40.0	517
0.416	0.256	70.2	196	49.3	282
0.154	0.250	71.9	223	66.1	101

Therefore, we believe that the VI NES mass m_2 should not be optimized. The mass value must be selected in advance, and all other parameters must be optimized for this selected mass. For example, in [19], the authors constructs the contour plots for each mass separately. In this paper, we analyze the efficiency and dynamic performance of the systems with attached SSVI NES and DSVINES of 4 different mass values: $m_2 = 60$ kg, 40 kg, 20 kg, and 10 kg, which are 6%, 4%, 2%, and 1% of the PS mass m_1 .

It is worth emphasizing that optimization procedures do not and cannot give the unambiguous result, since there are many sets of damper parameters that provide the similar minimal values of the objective function, that is, the similar mitigating the PS vibrations. This paper shows this very clearly. In the paper [12], the authors write: “*The nonlinear stiffness properties have significant influence on control effectiveness, and they can be implemented in numerous scenarios with plenty of configuration parameters.*” Besides, there is no rule or order for performing optimization procedures. In the article [13], the authors claim: “*There is no exact method to simplify the design of the multiparameter nonlinear energy sinks*”. The optimization of damper parameters requires a great experience and skill on the part of the researcher.

4. Dynamic behavior of the system with attached dampers of mass $m_2 = 60$ kg

This mass m_2 is 6% of the primary structure mass m_1 .

Optimization procedures allowed us to find five variants of the parameter sets for both SSVI NES and DSVI NES that provide good mitigation of the PS vibrations. Table 2 shows these parameters. The Table 2 also shows the values of the maximum total energy $E_{1\max}$ of the PS at the exciting force frequency $\omega = 6.3$ rad/s. This is the resonant frequency for the PS without any damper. In this case, the maximum total energy of the PS $E_{1\max} = 1557$ J. The rows with general title “Regimes” demonstrate the modes occurring in the system with different attached dampers. Hereinafter, the following notations are adopted. The designation nT, k, m indicates the nT -periodic mode (where T is the period of the harmonic exciting force) with k left impacts per cycle on the PS directly for the SSVI NES or on the left obstacle for the DSVI NES and m impacts on the right obstacle. For example, $2T, 1, 0$ is the regime of $2T$ periodicity with one impact per cycle on the left barrier and no impacts on the right obstacle. The AM designation indicates the amplitude-modulated mode, which will be discussed in detail below.

Table 2

Information about 5 variants of SSVI NES and DSVI NES of mass $m_2 = 60$ kg with optimized design

Parameters	Variant									
	SS-1(60)	SS-2(60)	SS-3(60)	SS-4(60)	SS-5(60)	DS-1(60)	DS-2(60)	DS-3(60)	DS-4(60)	DS-5(60)
k_2 , N/m	215	215	227	203	215	218	236	260	237	561
c_2 , N·s/m	232	232	152	83.6	250	247	214	108	209	32.8
$D(I)$, m	0.0600	0.0600	0.0697	0.759	0.0600	0.0636	0.0608	0.0598	0.635	0.0505
C , m	0.300	0.360	0.349	0.435	0.300	0.149	0.182	0.222	0.189	0.268
$E_{1\max}$, J at $\omega = 6.3$ rad/s	321	570	241	145	335	379	303	206	761	135
Regimes	$T, 0, 0$	$T, 0, 0$	$T, 0, 0$	$T, 0, 0$	$T, 0, 0$	$T, 0, 0$	$T, 0, 0$	$T, 0, 0$	$T, 0, 0$	$T, 0, 0$
	$3T, 1, 0$	$3T, 1, 0$	$3T, 1, 0$	$3T, 1, 0$	$3T, 1, 0$	$T, 1, 1$	$T, 1, 1$	$T, 1, 1$	$T, 1, 1$	$T, 1, 1$
	$2T, 1, 0$	$2T, 1, 0$	$2T, 1, 0$	$2T, 1, 0$	$2T, 1, 0$					
	$T, 1, 1$	$T, 1, 1$	$T, 1, 1$	$T, 1, 1$	$T, 1, 1$					
	AM	AM	AM	AM	AM					

Fig. 2 presents the dependence of the maximum total energy $E_{1\max}$ of the PS on the exciting force frequency for these five variants. Fig. 2 clearly demonstrates the good mitigation of the PS vibrations similar for SSVI NES and for DSVI NES. Below we take a closer look at some of the features of these options. Table 2 shows the presence of $T, 0, 0$ regimes for all damper variants. This is a shockless regime without any impact. Fig. 3 and Fig. 4 give a clear indication of where the impacts are occurring. The pink zones bounded by the vertical dashed lines in both Figures are areas where the bilateral impacts occur. These are the direct impacts on the PS for the SSVI NES and the impacts on the left obstacle for the DSVI NES and impacts on the right obstacles for both damper types. Table 2 shows

that the regimes with bilateral impacts are $T,1,1$ for both damper types. However, amplitude-modulated (AM) regime with bilateral impacts also occur for SSVI NES. The light green areas in Fig. 3 correspond to the areas where the unilateral direct impacts on the PS occur. The white areas in both Figures indicate shockless movement $T,0,0$.

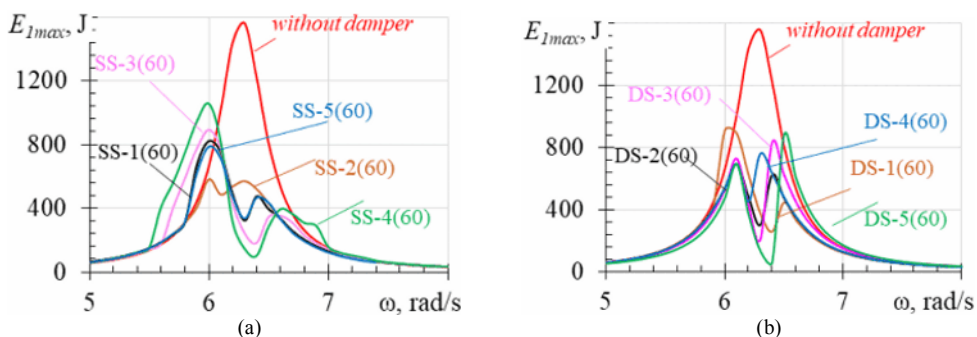


Fig. 2. The maximum total energy of the PS with different attached dampers of mass $m_2 = 60$ kg depending on the exciting force frequency: (a) for SSVI NES; (b) for DSVI NES

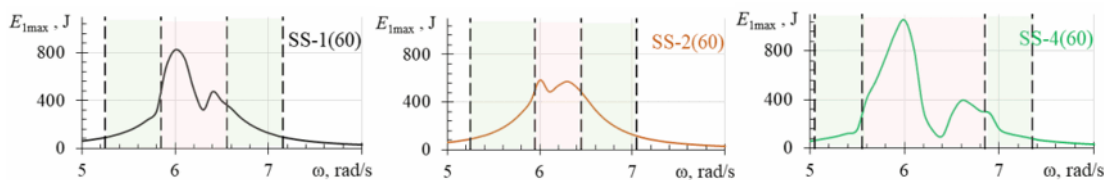


Fig. 3. The areas of bilateral and unilateral impacts for different single-sided vibro-impact nonlinear energy sinks with mass $m_2 = 60$ kg depending on the exciting force frequency

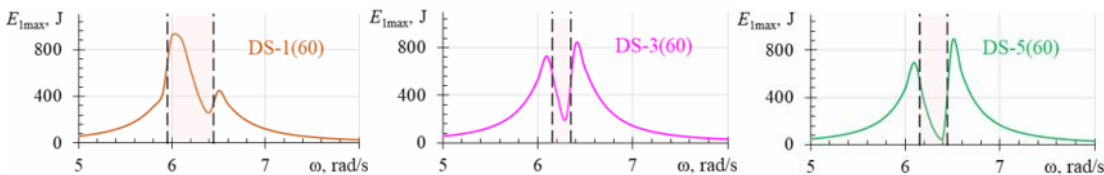


Fig. 4. The areas of bilateral and unilateral impacts for different double-sided vibro-impact nonlinear energy sinks with mass $m_2 = 60$ kg depending on the exciting force frequency

Fig. 5 shows the amplitude-modulated regime characteristics in detail. The upper envelope in red color in the plot of the time history of PS displacements is obtained using the Hilbert transform. Its frequency $\Omega = 0.31$ rad/s.

The analysis of the above allows us to formulate the following observations.

- Indeed, there is a lot of damper parameter sets that ensure the similar good mitigation of the PS vibrations. Table 2 and Fig. 2 clearly demonstrate this.

- A small changing in only one parameter can cause a significant change in the damper dynamics. Changing the clearance C in the variants SS-1(60) and SS-2(60) (see Table 2) gives a different motion picture (see Fig. 2).

- Attaching SSVI NES or DSVI NES to the PS does not change the behavior of the PS energy as a whole, which can be clearly seen in Fig. 2. However, the dynamics of the system movement is significantly different for these damper types. The “Regimes” rows in Table 2 show quiet movement with symmetrical impacts on both obstacles for the system with attached DSVI NES. In contrast, the system with attached SSVI NES demonstrates complex dynamics with both periodic and irregular motions. Fig. 5 presents the amplitude-modulated regime with bilateral impacts.

- It is important to emphasize that the bilateral impacts occur in rather narrow areas of the exciting force frequency located near the resonant one. For the system with DSVI NES attached, these areas are narrower, which can be clearly seen in Figs. 3 and 4.

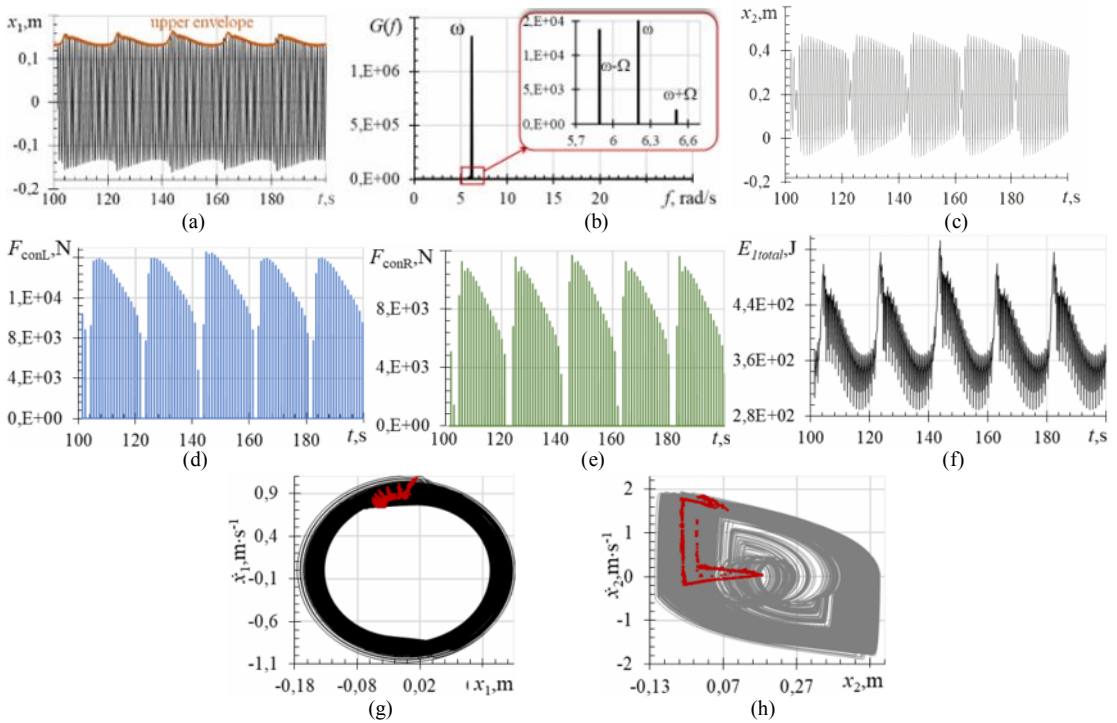


Fig. 5. Characteristics of the amplitude-modulated (AM) regime for the system with the damper of SS-2(60) variant at $\omega = 6.2$ rad/s. (a) The time history of the PS displacements. The frequency of the red upper envelope is $\Omega = 0.31$ rad/s. (b) Fourier spectrum for PS. (c) The time history of the damper displacements. (d) The contact impact forces at direct damper impacts on the PS. (e) The contact forces at damper impacts on the obstacle. (f) The total mechanical PS energy depending on time. (g) The phase trajectories and Poincaré map in red for PS. (h) The phase trajectories and Poincaré map in red for the damper

5. Dynamic behavior of the system with attached dampers of mass $m_2 = 40$ kg

The performance and dynamics of the system with DSVI NES and SSVI NES of mass $m_2 = 40$ kg attached to the PS have been discussed in detail in our previous work [18]. Optimization procedures allowed us to find several damper parameter sets that mitigate the PS vibrations well. In general, the pattern of the behavior of the PS energy is similar to that with dampers of mass $m_2 = 60$ kg. Fig. 6 shows the dependence of the maximum total energy of the PS with attached SSVI NESs and DSVI NESs of mass $m_2 = 40$ kg on the exciting force frequency.

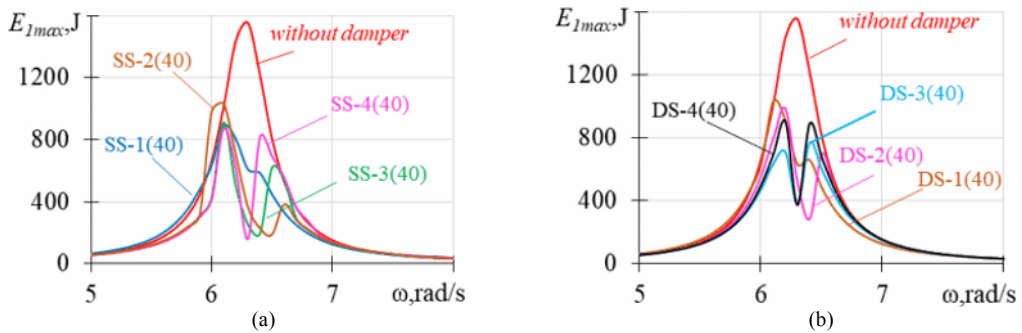


Fig. 6. Maximum total energy of the PS with different attached dampers of mass $m_2 = 40$ kg depending on the exciting force frequency; (a) for SSVI NES; (b) for DSVI NES

However, we observe a tendency to increase the clearance C and to decrease the damping coefficient c_2 especially pronounced for SSVI NES. Table 3 shows this trend.